Role of circ-FOXO3 and miR-23a in radiosensitivity of breast cancer

Abdollahi, Elahe; Mozdarani, Hossein; Alizadeh, Behrooz Z.

Published in:
Breast Cancer

DOI:
10.1007/s12282-023-01463-4

Publication date:
2023

Breast Cancer (2023) 30:714–726
https://doi.org/10.1007/s12282-023-01463-4

ORIGINAL ARTICLE

Role of circ-FOXO3 and miR-23a in radiosensitivity of breast cancer

Elahe Abdollahi[1] · Hossein Mozdarani[1] · Behrooz Z. Alizadeh[2]

Received: 28 November 2022 / Accepted: 25 April 2023 / Published online: 24 May 2023

Abstract

Identifying the radiosensitivity of cells before radiotherapy (RT) in breast cancer (BC) patients allows appropriate switching between routinely used treatment regimens and reduces adverse side effects in exposed patients. In this study, blood was collected from 60 women diagnosed with Invasive Ductal Carcinoma (IDC) BC and 20 healthy women. To predict cellular radiosensitivity, a standard G2-chromosomal assay was performed. From these 60 samples, 20 BC patients were found to be radiosensitive based on the G2 assay. Therefore, molecular studies were finally performed on two equal groups (20 samples each) of patients with and without cellular radiosensitivity. QPCR was performed to examine the expression levels of circ-FOXO3 and miR-23a in peripheral blood mononuclear cells (PBMCs) and RNA sensitivity and specificity were determined by plotting Receiver Operating Characteristic (ROC) curves. Binary logistic regression was performed to identify RNA involvement in BC and cellular radiosensitivity (CR) in BC patients. Meanwhile, qPCR was used to compare differential RNA expression in the radiosensitive MCF-7 and radioresistant MDA-MB-231 cell lines. An annexin -V FITC/PI binding assay was used to measure cell apoptosis 24 and 48 h after 2 Gy, 4 Gy, and 8 Gy gamma-irradiation. Results indicated that circ-FOXO3 was downregulated and miR-23a was upregulated in BC patients. RNA expression levels were directly associated with CR. Cell line results showed that circ-FOXO3 overexpression induced apoptosis in the MCF-7 cell line and miR-23a overexpression inhibited apoptosis in the MDA-MB-231 cell line. Evaluation of the ROC curves revealed that both RNAs had acceptable specificity and sensitivity in predicting CR in BC patients. Binary logistic regression showed that both RNAs were also successful in predicting breast cancer. Although only circ-FOXO3 has been shown to predict CR in BC patients, circ-FOXO3 may function as a tumor suppressor and miR-23a may function as oncomiR in BC. Circ-FOXO3 and miR-23a may be promising potential biomarkers for BC prediction. Furthermore, Circ-FOXO3 could be a potential biomarker for predicting CR in BC patients.

Keywords Breast cancer · G2 assay · Cellular radiosensitivity · Circ-FOXO3 · miR-23a

Introduction

Breast cancer (BC) is the most common cancer in women and the leading cause of cancer-related death in women worldwide [1]. Radiation therapy (RT) is commonly used as an adjuvant therapy in approximately 50% of all cancer patients at some stages of the disease [2]. However, some patients are over/undertreated after RT [3]. Radiosensitivity refers to the relative sensitivity of different cells (tissues, organs, or organisms) to the effects of ionizing radiation (IR) [4]. The radiosensitivity of cells depends on many factors, including the type of radiation and the ability to repair DNA, etc. [5]. Identifying radiosensitive patients before performing RT allows a proper alternation in routinely used treatment regimens to decrease the adverse side effects in exposed patients [4]. Although triple-negative breast cancer (TNBC) and Her2 + subtypes are nearly radioresistant, radiation response analysis of various breast cancer subtypes shows that luminal subtypes (A, B) are more radiosensitive. [6]. Given that different BC molecule subtypes respond differently to irradiation, this can affect the clinical outcome of treatment [7]. Studies have shown that peripheral blood lymphocytes in various types of cancer patients have higher levels of chromosomal abnormalities (CA) than in healthy

✉ Hossein Mozdarani
mozdarah@modares.ac.ir

[1] Department of Medical Genetics, Faculty of Medical Sciences, Tarbiat Modares University, Tehran, Iran

[2] Unit of Personalized Medicine, Department of Epidemiology, University Medical Center Groningen, Groningen, The Netherlands

people after irradiation [8]. An increase in CA after irradiation has been shown in about 40% of BC patients, but only in about 10% of healthy subjects [9, 10]. The G2 assay is a widely used method to study radiation sensitivity. In vitro irradiation of peripheral blood lymphocytes in the G2 phase of the cell cycle to induce DNA damage is often repaired during the G2-to-M transition, and residual lesions can be observed and measured at the metaphase as CA [11]. The high frequency of chromosomal aberrations that occur after G2 radiation exposure significantly distinguishes radiosensitive and non-radiosensitive cells or individuals [12–16]. Several reports have shown high frequencies of chromosomal aberrations in breast cancer lymphocytes after G2 exposure to IR [17–19]. IR used in RT induces different types of DNA damage such as double-strand breaks (DSBs) [20]. DNA double-strand breaks (DSBs) are dangerous form of damage that can lead to cell death and genome rearrangements. DSBs are repaired using two-component kinetics. In both phases, the fast process uses Canonical Nonhomologous End Joining (c-NHEJ) to repair most DSBs [21]. Chromatid aberrations in G2 may be induced following the signaling pathway induced by the initial induction of DNA damage [22, 23]. DNA Damage Response (DDR) plays an important role in DSB repair [24]. DDR maintains genomic stability by protecting cells from apoptosis and malignancies [25]. Circular RNAs (circRNAs) are novel endogenous non-coding RNAs (ncRNAs) characterized by a closed-loop structure [26]. A special structure that prevents exonuclease-mediated degradation makes circRNA highly stable, helping circRNA resist degradation by RNases and highlighting the advantages of circRNA as a stable molecular biomarker for various cancers [27–29]. CircRNA is also an important regulator in cancer biology [30–32]. CircRNA regulates the expression of related genes by specifically binding to microRNAs (miRNAs) as competing endogenous RNAs (ceRNAs) and functioning as miRNA sponges. [33]. miRNAs are small non-coding RNA subtypes of 20–25 nucleotides in length that have been identified for their role in the development of breast tumors and the regulation of radiation responses [27]. MiRNAs can affect tumor radiosensitivity through the regulation of the DDR [15].

Circular RNA Forkhead Box O3 (circ-Foxo3, hsa_circ_0006404) is encoded by the human FOXO3 gene [34]. Studies have shown that circ-FOXO3 is also involved in the inhibition of the progression of acute myeloid leukemia [35], glioblastoma [36], lung cancer [37], and breast cancer [38]. Several discoveries have been reported regarding the functionality of circ-FOXO3. Low levels of circ-FOXO3 have been demonstrated in breast cancer, but their expression has been shown to increase when cancer cells undergo apoptosis [39, 40]. Overexpression of circ-Foxo3 promotes cell apoptosis in bladder cancer [41], prostate cancer [42], and breast cancer [40]. On the other hand, the results showed that downregulation of circ-FOXO3 significantly increased post-irradiation DNA damage and apoptosis, whereas upregulation of circ-FOXO3 showed the opposite result. These data suggest that circ-FOXO3 is involved in radiation-induced cardiotoxicity [43]. However, the role of circ-FOXO3 in breast cancer radiosensitivity remains unclear. This non-coding RNA acts as a sponge for potential miRNAs. Studies have shown that circ-Foxo3 sponge miR-23a effectively suppresses esophageal squamous-cell carcinomas (ESCC) progression by upregulating PTEN expression [44]. Studies have revealed that DNA Topoisomerase 1 (TOP1) was identified as a direct target of miR-23a. This is essential for maintaining genomic stability during DNA damage. [45], and the inhibition of TOP1 by miR-23a led to a cellular topoisomerase activity that fell below the crucial critical threshold and induces cell death [46]. Functional analysis observed that the knockdown of miR-23a may reduce p53-induced apoptosis. These data show that miR-23a can promote the apoptotic effect of p53. [47]. Studies suggest that miR-23a promotes endothelial cell proliferation and migration as well by inhibiting the expression of PTEN, it promotes angiogenesis in radiation therapy [48, 49]. This is one of the causes of radiation resistance in lung cancer and may be a new target for increasing the sensitivity of radiation therapy [50]. MiR-23 and circ-FOXO3 expression levels in breast cancer radiosensitivity are largely unknown. We aimed to investigate the potential involvement of circ-FOXO3 and miR-23a in the radiosensitivity of lymphocytes and the apoptosis rate of breast cancer cell lines in IDC BC patients. To do this, a standard G2 assay was used to differentiate patients as radiosensitive and non-radiosensitive groups based on their cellular radiosensitivity. Then, for the first time, We studied the association of FOXO3 and miR-23a with cellular radiosensitivity in PBMC of BC patients. Next, we evaluated the expression levels of circ-FOXO3 and miR-23a in two radiation-resistant and radiation-sensitive cell lines. Finally, both cell lines were evaluated for cell apoptosis before and after irradiation. The ultimate aim of this study was to evaluate the potential use of the circular RNA and miRNA used in this study to predict cellular radiosensitivity and early detection of BC.

Materials and methods

Study population

BC patients with stage I / II invasive ductal carcinoma (60 women, average age 47 ± 9.92 years) were randomly selected at the Cancer Institute at Imam Khomeini Hospital (Tehran, Iran). Patients were selected among new-case individuals who had not received chemotherapy and/or primary radiotherapy or previous anticancer drugs before blood sampling.

They also had no history of using alcohol or drugs. First-degree relatives have no history of cancer and no signs of radiosensitivity-related congenital chromosomal disruption syndrome (including ataxia-telangiectasia, xeroderma pigmentosum, etc.). Age- and gender-matched healthy donors (20 females; mean age 44 ± 6.7 years) without prior history of breast cancer or other serious medical conditions in them or their first-degree relatives at the same time were also included as a healthy group. Factors such as diet, medical history, exposure to chemical and physical agents, smoking and alcohol/drug consumption, etc. were asked using a written questionnaire to obtain information on all lifestyles. Individuals with these confounders were excluded from the study for at least 1 month before blood collection. Informed consent was obtained from all patients and healthy participants, according to institutional ethics committee guidelines. This study was approved by the Ethics Committee of the Tarbiat Modares University (Registration no IR.MODARES.REC.1400.176 dated 10. October 2021).

Cell culture and G2 chromosomal radiosensitivity assay

Peripheral blood (2 ml) was collected in heparinized tubes from all participants. Each blood sample was divided into two parts: non-exposed and exposed to gamma irradiation. In brief, 0.5 ml of heparinized blood was added to 4.5 ml of complete RPMI-1640 (Bioidea, EU) supplemented with 10% fetal bovine serum (Bioidea, EU), penicillin (100 IU/ml), and streptomycin (100 µg/ml) (Bioidea, EU) and 100 µl phytohemagglutinin (Gibco, BRL, USA). Each culture vessel was prepared twice, one was checked for spontaneous chromatid break yield (SY) as a control, and the other was checked for induced chromatid break yield (IY) by gamma irradiation. The cell culture was incubated at 37° C for 72 h. Culture vessels were irradiated with a 1 Gy dose of gamma radiation generated by a 60 Co source (Theratron-II 780C, Kanata, Canada) at room temperature (4–5 h before harvesting) at a dose rate of 0.8–1 Gy. Colcemid (Gibco, BRL) was added at a concentration of 4 µg/ml, 1.5 h before harvesting to arrest cells at metaphase. Harvesting was done according to the standard procedures and slides were prepared and air-dried before staining with 4% Giemsa. To analyze metaphase, 100 well-spread metaphases were scored on slides before irradiation, and 100 lateral metaphases after irradiation were examined under a light microscope (Leica, Japan) for the presence of chromatid breaks in each sample. Evaluated at 1000 × magnification. The difference in chromatid break yield before and after irradiation was analyzed. The cut-off value for radiation-induced chromatid abnormalities in the lymphocytes of healthy subjects was defined as mean aberrations + 2SD, according to a study by Scott et al. [9, 15]. This method allows us to distinguish between patients with and without cellular radiosensitivity. Molecular studies have been conducted according to cellular radiosensitivity in BC patients. Figure 1 shows exemplary photomicrographs of metaphase cells with and without chromatid aberrations after irradiation of G2 lymphocytes.

Isolation of peripheral blood mononuclear cells (PBMC)

Two ml of peripheral blood was also collected from each sample into K2-EDTA tubes for molecular experiments. Blood samples were diluted with an equal volume of phosphate-buffered saline (PBS) and mixed. This solution was carefully added to 3 ml of Ficoll-Hypaque (Lymphodex Inno-Train) and centrifuged at 400 g for 40 min. The PBMCs were then carefully transferred to a new tube, further diluted with PBS, and centrifuged at 500 g for 15 min (twice). The RNA isolation procedure was performed immediately on the pellet according to the manufacturer's instruction.

Cell culture and Irradiation

Breast cancer cells, MCF-7, and MDA-MB-231 cells were cultured at 1×10^6 cells/well in 6-well plates in DMEM medium (Gibco-BRL) supplemented with 10% fetal bovine serum (FBS) and antibiotics (Penicillin (100 IU/ml)/Streptomycin (100 µg/ml)). Ten minutes before irradiation, the medium was replaced with a fresh complete medium to provide proper backscatter. Cells were then exposed to 2 Gy, 4 Gy, and 8 Gy megavoltage X-rays generated from a 6-MV linear accelerator (LINAC) (Elekta, Sweden) at room temperature. Control cultures received no irradiation.

Apoptosis detection by Annexin V-FITC/PI binding assay

Both cell lines (MDA-MB-231 and MCF-7 cells) were incubated for 24 and 48 h after irradiation. Target cells were then detached using EDTA-free trypsin, and serum-containing

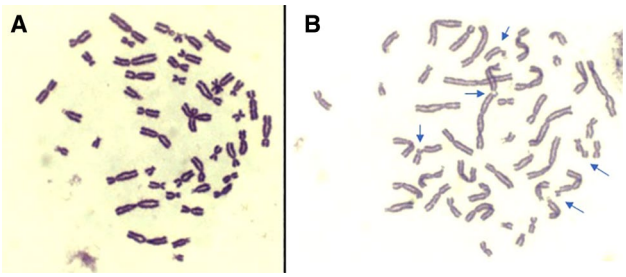

Fig. 1 Examples of abnormalities seen in metaphase **A** Normal metaphase, **B** Metaphase with chromatid breaks and deletions shown with arrows. Magnification × 1000

DMEM was used to neutralize trypsin. Cells were then washed with a 500 µl flow buffer. After washing, 5 µl of annexin V-fluorescein isothiocyanate V/FITC and 5 µl of propidium iodide (PI) were added to the tubes with target cells and incubated for 15 min at room temperature in the dark. Finally, cell apoptosis was analyzed using a FACSCalibur flow cytometer (BD Biosciences, CA).

RNA isolation and qRT-PCR

Total RNA was extracted from PBMCs and cell lines and TRIzol reagent (Invitrogen, Karlsruhe, Germany) was used according to the manufacturer's instructions. The purity and concentration of RNA samples were determined using a NanoDrop ND-1000 (Thermo Fisher Scientific, Wilmington, DE). For validation experiments, RNA was prepared and stored at −80 °C. For the synthesis of cDNA, we used the qPCRBIO cDNA synthesis kit and followed the protocol according to the manufacturer's instructions. The stem-loop primer was used to perform reverse transcription. Stem-loop primer sequences used in this study were as follows: hsa-miR-23a. 5′ GTCGTATCCAGTGCAGGGTCCGAGGTA TTCGCACTGGATACGACAAATCC 3′

The following reagents: miRNA, Stem-Loop RT primer (1 pM), and RNase-free water were gently mixed on ice and incubated at 70 °C for 5 min. Then, a mixture containing: ×5 first strand buffer, dNTP (10 mM each), and RNasin (40-MLV) was prepared, the mixture was then added to the tube, and then incubated at 16 °C for 30 min and 60 °C for 42 min using PCR system (Eppendorf). Termination of the reaction was performed using a 5-min incubation at 70 °C. Real-time PCR was performed using SYBR Green qPCR Mix Reagent (BIOFACT, Taiwan) on a real-time PCR system "Applied Biosystems, Step One Plus, USA". The sequences of the specific primers are shown in Table 1.

The universal reverse primer used was a 20 µl PCR reaction mix containing 2 × SYBR Green qPCR mix reagent (BIOFACT, Taiwan), forward and reverse primers (10 pM each), cDNA product, and nuclease-free water. The PCR reaction was incubated at 95 °C for 10 min, followed by 40 cycles of 95 °C for 15 s, 60 °C for 30 s, and finally 72 °C for 10 s. All reactions were performed in duplicates. Finally, we used Method 2 to analyze the relative expression levels of each RNA. All experiments were performed in duplicate.

Statistical analysis

For the G2 assay, the SY of the chromatid breaks was subtracted from the IY of each sample to obtain the radiation-induced yield (RIY). Results were analyzed using SPSS software (version 25, Chicago, USA). An unpaired t-test was used to compare the frequency of chromatid aberrations between groups before and after irradiation.

The normality of data distribution was examined using the Shapiro–Wilk test. Outliers were excluded from the analysis, and sampling was repeated. The association between circular RNA and miRNA expression levels and breast cancer was assessed by an unpaired t-test (comparison of the two groups). The association between radiosensitivity and miR23a and circ-FOXO3 expression was analyzed using Tukey's post hoc one-way ANOVA (comparing two or more groups). In addition, the nonparametric Kruskal–Wallis test (k samples) was also performed to determine significant differences between molecular subtypes of BC. $P < 0.05$ was considered a significant value. Meanwhile, Tukey's post hoc one-way ANOVA statistical test was used to examine RNA expression in two cell lines.

ROC curves were constructed to assess the accuracy of the use of miRNA and circular RNA in the detection of breast cancer and cellular radiosensitivity of BC patients. To evaluate the predictive values of these molecules, we calculated the area under the curve (AUC) for the ROC curve and the 95% confidence interval (95% CI). Finally, binary logistic regression was used to assess the ability of miRNA and circular RNA in predicting BC and cellular radiation responses.

Results

Patient demographic information and relevant pathological characteristics such as ER, PR, Her2, Ki67 status, lymph node status, and clinical stage are presented in Table 2. Pathologic information for some patients was not available.

The G2 assay analysis

The G2 assay was performed on lymphocytes collected from the blood samples of 60 BC women (group) and 20 healthy,

Table 1 Primer sequences used for Real-Time PCR

Target	Forward	Reverse
circ-FOXO3	5′TTGAACGTGGGGAACTTCAC3′	5′TCGACTATGCAGTGACAGGT3′
miR-23a	5′GATAGGGGTTCCTGGGGATG3′	5′AATACCTCGGACCCTGCAC3′
U6	5′CTCGCTTCGGCAGCACA3′	5′AACGCTTCACGAATTTGCGT3′
GAPDH	5′ATGAGAAGTATGACAACAGCCTC3′	5′CATGAGTCCTTCCACGATACC3′

Table 2 Demographic information of included patients

Category	Number	Percentage
(%)		
Age (years)		
< 40	18	30
41 54	27	45
> 55	15	25
T Stage[a]		
T1 ≤ 2 cm	24	40
T2		
T3 > 2 cm	36	60
Lymph node status[b]	21	35
Positive	39	65
Negative		
Clinical TNM staging		
I	17	27.5
II	43	72.5
ER/PR/HER2 status		
ER + /PR + /HER2-	16	27.5
ER + /PR-/HER2-	10	17.5
ER-/PR + /HER2-	9	15
ER-/PR-/HER2 +	3	7.5
ER + /PR + /HER2 +	7	12.5
ER-/PR-/HER2-	9	20
The mean level of ki-67[c]		
(Luminal A) ≤ 14	14	39.13
(Luminal B) > 14	21	60.87

[a]T0 = no evidence of primary tumor, T1 = tumor 2 cm, T2 = tumor > 2 cm not exceeding 5 cm,

T3 = tumor > 5 cm, T4 = tumors with metastasis to surrounding tissues that were not included in our study

[b]positive = metastasis to axillary lymph nodes and or in internal mammary nodes, negative = no regional lymph node metastasis histologically, no additional examination for isolated tumor cells

cER + /PR + /HER2-, ER + /PR-/HER2-, and ER-/PR + /HER2- are considered as BC luminal subtypes. The mean level of ki-67 is usually determined to differentiate luminal A from Luminal B

gender-matched individuals with or without 1 Gy of gamma irradiation.

The SY was 1 ± 0.78 and 3.35 ± 1.90 in metaphase related to the lymphocytes of healthy individuals and patients respectively (unpaired t-test; $p = 0.009$). The patient's irradiation yield IY was also significantly different from the control. The mean RIY was 2.95 ± 1.5 per 100 cells in the control group and 7.6 ± 4.8 in patients, which was significantly higher in patients (unpaired t-test, $p = 0.001$). No significant difference in mean age between these two groups was observed (unpaired t-test, $p = 0.0699$). Cut-off values were obtained to classify individuals into cellular radiosensitive and non-cellular radiosensitive groups using the mean number of induced chromatid abnormalities + 2 SD observed according to the method used in the study carried out by Scott et al. [17]. The results are shown in Fig. 2A and B.

Based on the determined cut-off value, lymphocyte cultures from patients were divided into two groups, with cellular radiosensitivity and without cellular radiosensitivity. From 60 lymphocyte cultures initiated from BC patients and irradiated at G2, 32 lymphocyte cultures (53.33%) showed cellular radiosensitivity, and 28 cultures (46.66%) were found without cellular radiosensitivity. From these 60 samples, 20 were selected that were more radiosensitive, and 20 were less radiosensitive than the rest. Therefore, molecular studies were finally performed on 40 BC patients, including 2 equal groups (20 samples each) of patients with and without cellular radiosensitivity.

Association of circ-FOXO3 and miR-23a with BC and cellular radiosensitivity

According to the circBase dataset, hsa_circ_0006404 is derived from the FOXO3 gene on chromosome 10, which is the result of exon 2 back splicing. For convenience, this circRNA is called circ-FOXO3 (Fig. 3). Circ-FOXO3 was significantly down-regulated in PBMCs extracted from 40 BC patients compared to samples taken from 20 healthy subjects (expression ratio = 0.252, unpaired t-test, < 0.0001). On the other hand, the expression of miR-23a was increased in 40 BC samples compared to 20 healthy subjects (expression ratio = 4.06, unpaired t-test, $p < 0.0001$; (Fig. 4A,B). Expression of circ-FOXO3 was directly related to cellular radiosensitivity. The expression of this circular RNA was reduced in leukocytes from samples with cellular radiosensitivity (expression ratio = 0.38) and without cellular radiosensitivity (expression ratio = 0.11) compared with leukocytes in the control group. In addition, the circ-FOXO3 expression was significantly higher in the cellular radiosensitive group than in the non-cellular radiosensitive group (expression ratio = 3.45). After running the Tukey Post Hoc One-way ANOVA test, we found that these observations are statistically significant with respective $p = 0.07$, $p < 0.0001$, $p = 0.01$; Fig. 4C). Analysis of miR-23a expression in our three research groups showed that it was also directly associated with cell radiosensitivity in BC patients. Comparing samples with and without cellular radiosensitivity to controls showed an increase in the miR-23a expression ratio of 3.2 and 7.87, respectively. A lower level of miR-23a expression was observed in the radiosensitive samples compared to the non-radiosensitive samples (expression ratio = 0.4). Based on non-parametric ANOVA test results were statistically significant with $p = 0.02$, < 0.0001, and < 0.01 respectively (Fig. 4D).

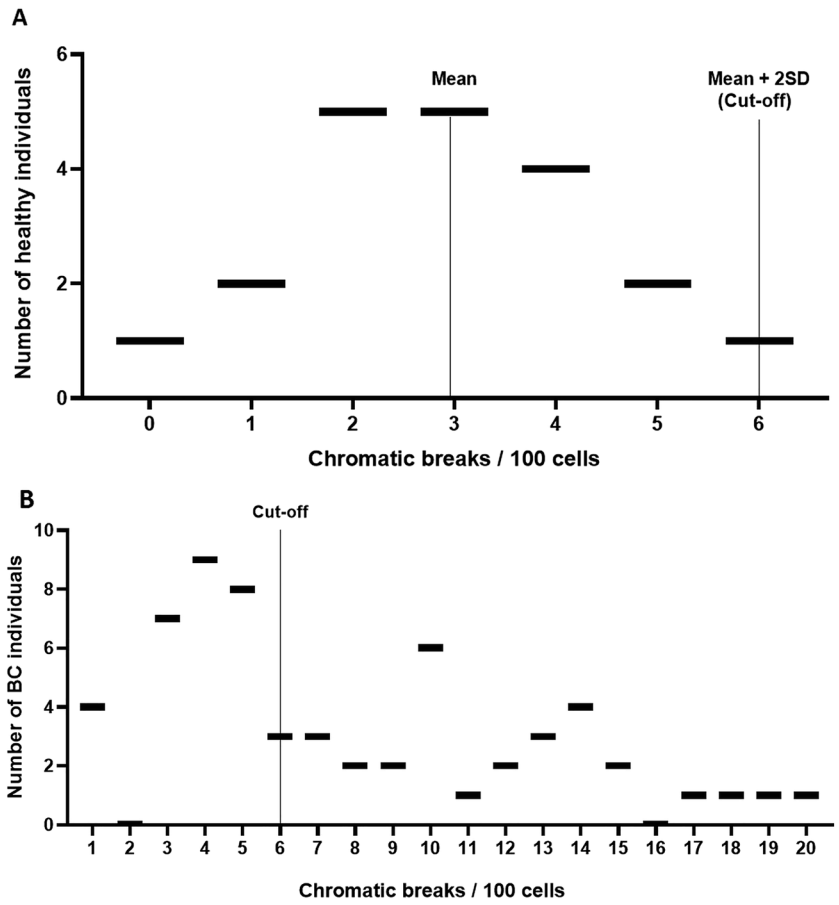

Fig. 2 Cut-off values to classify the cells as radiosensitive and non-radiosensitive **A** Distribution of radiation induced chromatid breaks frequency in cells of healthy individuals (n = 20) and **B** breast cancer patients (n = 60). Dashed lines indicate the mean + 2 SD used to indicate the cut-off point

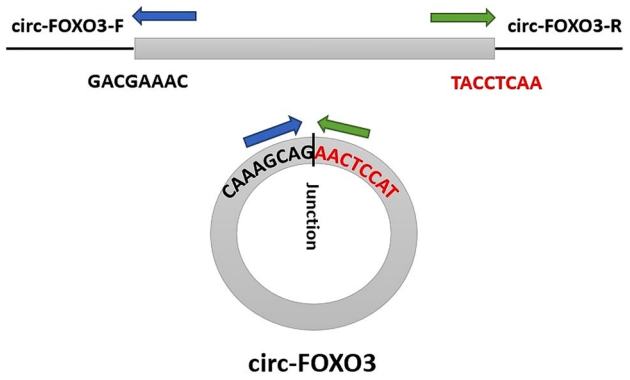

Fig. 3 Scheme illustrating the production of circ-FOXO3 and sequencing analysis of back-splicing junction in circ-FOXO3

Predictive values of circ-FOXO3 and miR-23a in cellular radiosensitivity in BC patients

Since both circ-FOXO3 and miR-23a were differentially expressed in BC and healthy samples, ROC curves were applied to assess the specificity and sensitivity of these RNAs in distinguishing between BC patients and healthy subjects. For circ-FOXO3, a sensitivity of 85%, a specificity of 70%, an AUC value of 0.8706 (0.7726–0.9687; $p < 0.0001$), and a confidence interval of 95% were obtained (Fig. 5A).

Analysis of the ROC of miR-23a showed 82.5% sensitivity, 70% specificity, and an AUC value of 0.838 (0.7389–0.9386; $p < 0.0001$). (Fig. 5B).

The ROC curve was also used to assess the predictive power of the mentioned RNA for cellular radiosensitivity in BC patients. Regarding the radiation response, the AUC value was 0.825 (0.699–0.950; $p = 0.0004$) 95% CI, sensitivity of 55%, and specificity of 100% for circ-FOXO3 (Fig. 5C) and 0.74 (0.5852–0.8948; $p = 0.009$) with a sensitivity of 70% and specificity of 75% for miR-23a (Fig. 5D). Binary logistic regression analysis was applied to predict the ability of circ-FOXO3 and miR-23a in predicting breast cancer and its cellular radiosensitivity. The results for circ-FOXO3 were with an odds Ratio = 0.06 ($p = 0.02$) and with an odds Ratio = 1.683 ($p = 0.001$) for miR-23a in BC predication. Regarding radiation response analysis, binary logistic regression evaluation showed that only circ-FOXO3 could predict cellular radiosensitivity in BC patients with $p = 0.04$ and odds ratio = 0.81, whereas miR-23a did not ($p = 0.06$). The evaluated results demonstrated that miR-23a was a positive factor in predicting BC

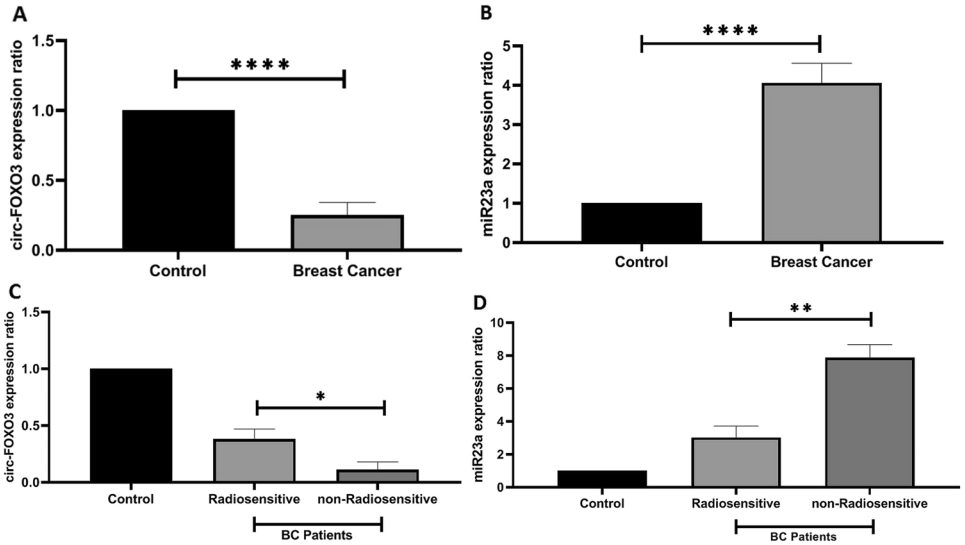

Fig. 4 Studied RNAs analysis in BC **A** circ-FOXO3 is down-regulated in breast cancer (40 individuals) compared with healthy individuals (20 individuals). **B** MiR-23a expression level is increased in breast cancer (40 individuals) versus healthy control (20 individuals). miR-23a and circ-FOXO3 expression levels and BC cellular radiation response. **C** The BC group without cellular radiosensitivity showed a lower expression level of circ-FOXO3. **D** The BC group with cellular radiosensitivity showed a lower expression of mentioned miR-23a compared to the BC group without cellular radiosensitivity. *p < 0.05; **p < 0.01; ****p < 0.001

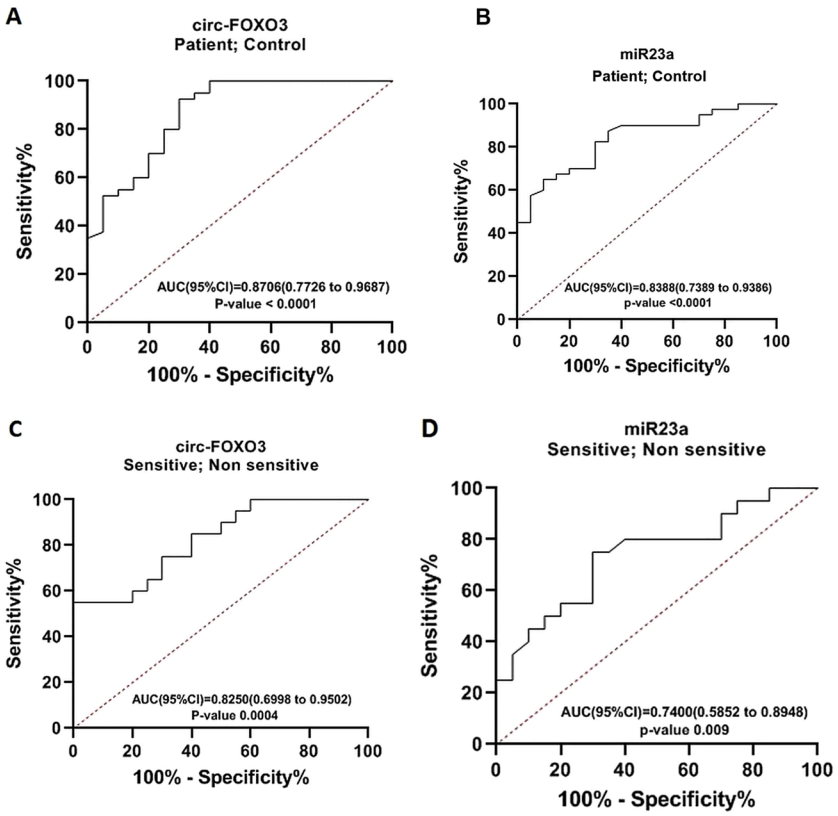

Fig. 5 ROC curve analysis **A** and **B** represent the ROC curves of the circ-FOXO3 and miR-23a in breast cancer (n = 40) compared to healthy controls (n = 20) **C** and **D** represent ROC curves of the circ-FOXO3 and miR-23a in patients with cellular radiosensitivity (n = 20) compared to patients without cellular radiosensitivity (n = 20))

and circ-FOXO3 was a negative factor in predicting BC and cellular radiosensitivity.

Chromatid breaks frequency in BC molecular subtypes

After determining the molecular subtypes of some patients based on pathological reports, it was found that 57.5% of BC cases were HR-positive (Luminal A + B), 20% were triple negative (TN), and 7.5% were HER2 + .

Based on the results from innate chromosomal aberration analysis (without irradiation) it was found that TN and HER2 + BC subtypes encompass higher mean of chromatid breaks frequency (CBF) compared to luminal A and B subtypes (3.67 ± 1.94 and 5.33 ± 1.73 vs. 3.07 ± 2.34 and 3.33 ± 1.40 respectively). Luminal A showed the lowest

CBF among all examined subtypes. To assess the Radiation Response Score (RRS) among BC subtypes, induced CBF was divided by spontaneous CBF values. Comparing radiation-induced and spontaneous chromatid breaks revealed the highest and lowest RRS for Luminal-B (3.84 ± 2.74) and HER2 + (2.05 ± 1.53), respectively. More details are presented in Supplemental Table 1.

Association of circular RNA and miRNA expression ratios with BC molecular subtypes

A nonparametric Kruskal–Wallis test (k sample) was performed to assess the association between circ-FOXO3 and miR-23a expression levels and molecular BC subtypes. Expression levels of the circular RNA and miRNA were compared with control groups for each BC molecule subtype an "Expression Ratio" vs. "Control" in Table 3. The expression levels of studied RNAs were compared in triple-positive (TP) vs. TN, luminal vs. HER2-positive, and luminal A vs. luminal B, and the results obtained are reported in Table 3 as "intergroup ratios." These values indicate the degree of expression change in each group compared to the other groups. For example, TPs tended to express circ-FOXO3 higher than the TN group (9.2-fold). In summary, for circ-FOXO3, a significant reduction in expression level differences was observed in all the BC molecular subtypes except for TP subtypes, compared to the control, and for miR-23a a significant increase in expression level differences was observed in all of the BC molecular subtypes except for TP and Luminal A subtypes compared to control (Kruskal–Wallis test; $p < 0.001$). More details are presented in Table 3.

Association of circ-FOXO3 and miR-23a with BC and the response of BC cells to IR

The expression levels of circ-FOXO3 and miR-23a were evaluated by qRT-PCR in MCF-7 and MDA-MB-231 cells irradiated with 2 Gy, 4 Gy, and 8 Gy X-rays. The expression level of circ-FOXO3 in MCF-7 at doses of 4 Gy and 8 Gy showed a significant increase compared to controls at both 24- and 48-h sampling times. Based on Tukey Post Hoc, one-way ANOVA test results were significant with $p = 0.018$, $p = 0.003$, $p = 0.0001$, and $p < 0.0001$ respectively. Comparison of the expression of this RNA in two cell lines showed that in doses at 4 Gy and 8 Gy, there is an increase expression in the MCF-7 cell line compared to the MDA-MB-231 cell line after 24- and 48-h using Tukey Post Hoc, One-way ANOVA test was significant with $p = 0.004$, $p < 0.0001$, 0.0006 and $p < 0.0001$ respectively.

Comparing the expression level of circ-FOXO3 at 24 and 48 h showed a significant difference in the MCF-7 cell line at 8 Gy ($p = 0.0001$) (Fig. 6A). On the other hand, miR23a expression increase was observed with increasing radiation dose in 4 Gy and 8 Gy after 24 h and in 2G, 4 Gy, and 8 Gy after 48 h in comparison to control in the MDA-MB-231 cell line. Based on Tukey Post Hoc, One-way ANOVA test results were significant with $p = 0.0008$, $p < 0.0001$, $p = 0.001$, $p = 0.0003$, and $p < 0.0001$ respectively. Also, the

Table 3 RNA expression ratios based on BC molecular subtypes

	BC molecular subtypes	Sample size	Expression ratios vs. control	p-value[a]	Inter-group ratios[b]	p-value
circ-FOXO3	1. Triple positive	5 (12.5%)	0.46	0.21	9.2	0.46
	2. Triple negative	8 (20%)	0.05	< 0.0001		
	1. Luminal	23 (57.5%)	0.38	0.01	2	> 0.999
	2. HER2 positive	3 (7.5%)	0.19	0.01		
	1. Luminal A	9 (22.5%)	0.46	0.01	8.75	> 0.999
	2. Luminal B	14 (35%)	0.3	< 0.0001		
miR-23a	1. Triple positive	5 (12.5%)	2.49	0.09	0.3	> 0.999
	2. Triple negative	8 (20%)	8.18	< 0.0001		
	1. Luminal	23 (57.5%)	2.9	0.007	0.22	0.39
	2. HER2 positive	3 (7.5%)	12.79	0.0009		
	1. Luminal A	9 (22.5%)	2.02	> 0.999	0.58	> 0.999
	2. Luminal B	14 (35%)	3.79	0.001		

Abbreviations: n = number of patients; TNM stage = tumor size; lymph nodes involvement; metastasis; ER = estrogen receptor; HER2 = human epidermal growth factor receptor; PR = progesterone receptor

[a]Kruskal-Wallis Non-parametric 2 independent samples test was performed, *statistically significant $p < 0.05$

[b]to obtain the expression ratio of RNAs in each group, the average of RNA expressions in group 1 was calculated and then divided by group 2, for example, the expression level in TP (group1) was divided by Triple Negative (group 2)

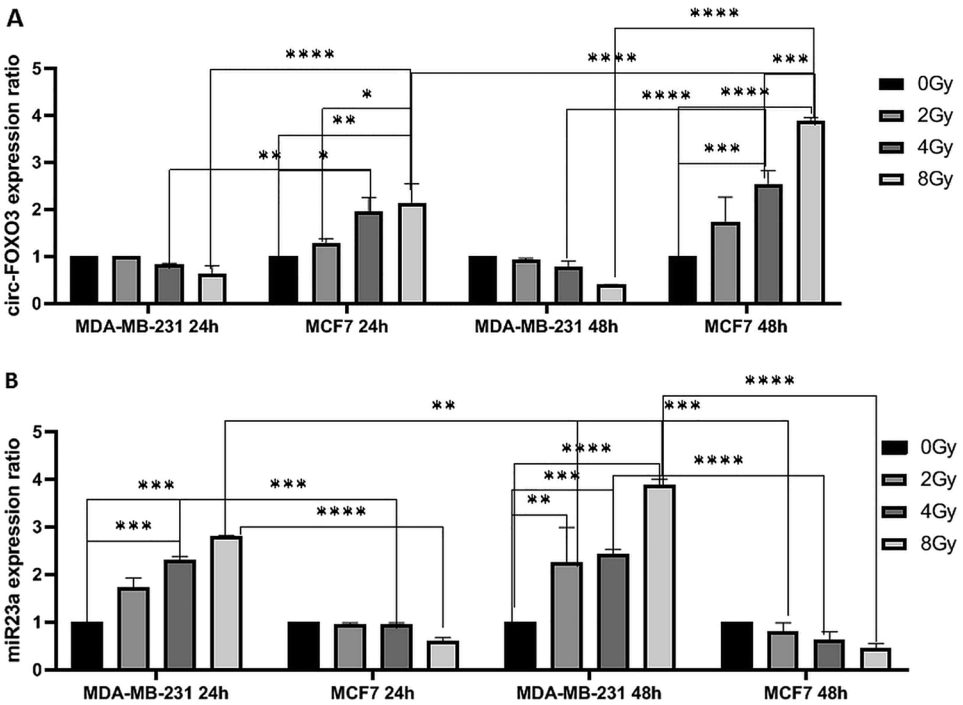

Fig. 6 **A** Comparison of the expression level of circ-FOXO3 among control and (2 Gy, 4 Gy, and 8 Gy) radiated MCF-7 and MDA-MB-231cell lines after 24 and 48 h. **B** Comparison of the expression level of miR23a among control and (2 Gy, 4 Gy, and 8 Gy) radiated MCF-7 and MDA-MB-231cell lines after 24 and 48 h. *p < 0.05; **p < 0.01; ***p < 0.001; ****p < 0.0001

comparison of the two cell lines showed that the expression of miR23a in 4 Gy and 8 Gy after 24 h, 2 Gy, 4 Gy, and 8 Gy after 48 h in the MDA-MB-231 cell line was higher than the MCF-7 cell line significantly different with p = 0.0005, p < 0.0001, 0.003, p < 0.0001 and p < 0.0001 respectively. The expression level of miR23a was significantly higher in the 8 Gy irradiated MDA-MB-231 cell line after 48 h compared to 24 h sampling time (p < 0.0001) (Fig. 6B).

Apoptosis data revealed that the apoptosis rate of MCF-7 cell lines exposed to 4 Gy and 8 Gy was significantly higher than in controls at 24 h (p = 0.0002 and 0.0005, respectively). The results also showed that the percentage of apoptotic cells was significantly increased at cells receiving 8 Gy after 24 h and 4 Gy and 8 Gy after 48 h compared to the control (p = 0.0002, p = 0.0005, p < 0.0001 respectively). The results also showed that cellular apoptosis was significantly higher in the MCF-7 cell line than in the MDA-MB-231 cell line at doses of 8 Gy at 24 h, 4 Gy, and 8 Gy at 48 h (p = 0.007, p = 0.013 and p = 0.004, respectively) (Fig. 7A and B).

Discussion

A possible prospect for radiosensitivity research is the creation of risk models involving genetic assays that can predict a patient's radiation response and the likelihood of developing radiation-induced side effects (4). This risk model can ultimately be combined with current predictors of radiosensitivity, such as radiation dose, the presence of other diseases

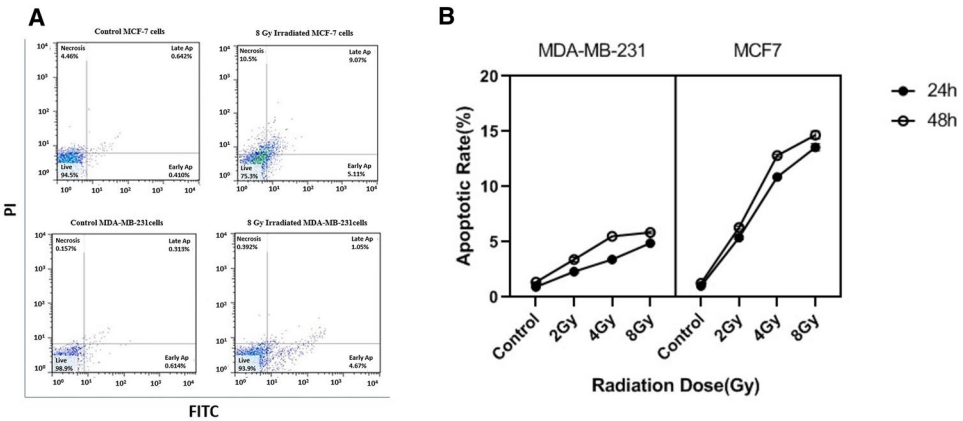

Fig. 7 Early and late apoptosis detection by flow cytometry assay through annexin V and PI staining. MCF-7 and MDA-MB-231cells were exposed to 2, 4, and 8 Gy x-radiation for 24 h and 48 h and then were subjected to the assessment by flow cytometry). MCF-7 cells were treated with medium only without radiation as a control. Control (**A**). The apoptotic rate of MCF-7 and MDA-MB-231 cells after irradiation and control (**B**)

and conditions in addition to primary cancer, and the amount of target exposed to radiation [51].

The results of the G2 assay suggest that SY is more common in patients than in controls ($p < 0.05$). We also noted that IY tended to be higher in the BC group than in the control group (Fig. 2). This result is consistent with some previous findings [9, 10, 18, and 53]. In addition, RIY scores were significantly higher in BC patients than in healthy subjects. On the other hand, the patient's lymphocytes were more sensitive to ionizing radiation than the lymphocytes of healthy subjects. Inter-individual differences in chromosomal radiosensitivity between BC patients and healthy individuals have also been observed [52]. These results are consistent with several previous studies on BC [9, 10, 18, 19, 53–55]. Deregulation of circular RNAs and miRNAs has been demonstrated in several cancers, including BC [56]. Studies have shown that some cancers, such as BC, have reduced levels of circ-FOXO3 expression [57]. As shown in Fig. 4A, Circ-FOXO3 was significantly down-regulated with BC-derived PBMCs (0.25 times). This was consistent with the study by Yang et al. [25]. Based on our results and according to the fact that circ-FOXO3 expression is reduced in several types of cancers [38, 41, 57–60], it can be concluded that circ-FOXO3 might probably act as a tumor suppressor circular RNA in breast cancer and may be a putative biomarker for early detection of BC. Based on the results of the present study as shown in Fig. 4C, the expression level of circ-FOXO3 was significantly higher (3.45-fold) in the radiosensitive group than in the non-radiosensitive group, which may be due to restraining DNA damage repair by circ-FOXO3 overexpression.

Our cell line results also demonstrated that the overexpression of circ-FOXO3 in the MCF-7 cell line, which is a radiation-sensitive cell line, is parallel to the increase in the radiation dose and the increase in cell apoptosis. Moreover, the expression of circ-FOXO3 in doses of 4 Gy and 8 Gy after 24 and 48 h is higher in the radiosensitive MCF-7 cell line than in the radiation-resistant MDA-MB-231 cell line. Our findings are consistent with the results of Qiu et al. demonstrating an association between circ-FOXO3 and radiosensitivity [43].

Furthermore, our data revealed that miR-23a expression is significantly (4.06 times) upregulated in PBMC in BC patients, consistent with relevant BC studies [61, 62]. So, it can be concluded that miR-23a may act as an oncomiR in BC and might be serve as a suitable potential biomarker of BC detection in its early stages. Exposure to ionizing radiation significantly alters RNA expression patterns in normal cells as well as in cancer cells [49, 63]. Studies have shown that overexpression of miR-23a can significantly increase the number of chromatid breaks compared to control cells [64]. Moreover, the expression level of miR-23a was significantly lower (0.4 times) in the radiosensitive group than in the non-radiosensitive group, which is in line with other reports [49, 63]. Although the AUC of the ROC curve is good for the association of miR-23a with blood radiosensitivity, the logistic regression is not statistically significant, so the most likely reason for this event is the sample size.

Our cell line results also showed the increased expression of miR-23a in the MBA-MD-231 radioresistant cell line, in parallel with increasing radiation dose. Furthermore, the expression of miR-23a at doses of 4 Gy and 8 Gy after 24 h and 2 Gy, 4 Gy, and 8 Gy after 48 h was higher in radioresistant MDA-MB-231 cell lines than in radiosensitive MCF-7. Our findings are consistent with the results of Chen et al., demonstrating an association between miR-23a and radiosensitivity [43, 48].

Based on the results obtained, the altered expression of these two RNAs can be considered potential biomarkers of cellular radiosensitivity in BC patients. This may help physicians more efficiently identify radiosensitive patients before RT in the future. This needs to be confirmed in clinical trials. Plotting ROC curves for circ-FOXO3 and miR-23a also indicated an acceptable specificity and sensitivity for distinguishing BC from healthy individuals (Fig. 5A and B). Moreover, both circ-FOXO3 and miR-23a were able to the separation of radiosensitive lymphocytes of BC patients from non-radiosensitive ones with a suitable specificity and sensitivity (Fig. 5C and D).

Binary logistic regression also confirmed the ability of circ-FOXO3 and miR-23a to identify BC patients from healthy volunteers. Both RNAs can predict BC, with the difference that miR23a is likely to be a positive factor and circ-FOXO3 is likely to be a negative factor in BC predictions. In cellular radiosensitivity assays, only circ-FOXO3 was sufficiently potent to successfully predict the radiosensitivity of BC-derived lymphocytes.

Comparing spontaneous CBFs among different BC subtypes revealed that the HER2 + and TNBC subtypes were more likely to have higher CBFs than the luminal subtypes. The obtained results seem logical, as both HER2 + and TNBC patients have a poor prognosis and luminal patients have a good prognosis. The Luminal-A group was found to have the lowest spontaneous CBF among all the studied groups. Given that the Luminal A group generally has a better prognosis than other subtypes and responds better to RT, the found results are consistent with our expectations. Furthermore, analysis of the radiation response revealed that among all subtypes, Luminal-B had the highest (3.84time) and HER2 + had the lowest (2.05 time) radiation response. Our data showed that the number of non-radiosensitive patients in the TN group was higher than that of radiosensitive patients. Inhibition in luminal-A and -B subtypes, most members were radiosensitive [65]. These results are consistent with several studies [71]. Previous studies of BC subgroups show that

the triple-negative and HER2-positive subgroups have a worse prognosis than the luminal subgroups [66–68].

As shown in Table 3, analysis of the RNA expression ratios in different BC molecular subtypes compared to healthy individuals revealed that circ-FOXO3 showed higher expression in BC molecular subtypes with a better prognosis. Our findings are consistent with previous studies suggesting that circ-FOXO3 acts as a tumor suppressor in some cases [57, 69, 70]. Analysis of miR-23a expression ratios in different BC molecular subtypes compared with healthy subjects revealed higher expression in BC molecular subtypes with poor prognosis. In agreement with several studies, miR-23a can function as an oncomiR in some cases [38]. Based on clinicopathologic information from participants in each group studied, the number of individuals in each subtype was not necessarily equal. To obtain more accurate results in association studies of these RNAs with BC subtypes, investigation of radiosensitivity-related RNA expression levels in larger sample sizes might be deemed necessary. Further clinical studies are recommended to derive clinical utility from these results. In conclusion, we suggest that the downregulation of circ-FOXO3 and upregulation of miR-23a may act as a tumor suppressor and oncogene RNA, respectively, in BC. Circ-FOXO3 and miR-23a can be considered potential biomarkers in BC detection. Both RNAs are involved in cellular radiosensitivity and thus may be promising potential biomarkers in determining cellular radiosensitivity in BC patients in vitro. This should be confirmed in other clinical studies for future BC radiosensitivity detection applications.

A limitation of this project was the sample size, possibly due to this, a small but non-significant difference was observed between the ages of control and patient subjects ($p = 0.0699$). Therefore, it is proposed to run this project with more samples.

Supplementary Information The online version contains supplementary material available at https://doi.org/10.1007/s12282-023-01463-4.

Acknowledgements This research was supported by the research department of the Faculty of Medical Sciences of Tarbiat Modares University, Tehran, Iran. The authors sincerely appreciate the head and staff of the Oncology Department of Imam Khomeini Hospital for their valuable cooperation. The authors also thank all patients and healthy volunteers who participated in this study. We also thank Mr. H. Nosrati for the irradiation of blood and cell line samples.

Author contributions All authors contributed to the study's conception and design. Supervision and study design [HM]. Material preparation, data collection, and analysis were done by [EA], and [HM]. The first draft of the manuscript was written by [EA] and editing was performed by [BA and HM]. All authors commented on previous versions of the manuscript. All authors read and approved the final manuscript.

Funding This research was supported by a grant (Grant Number: IG-39711) from the research department of the Tarbiat Modares University, Tehran, Iran.

Data availability Data would be available on request.

Declarations

Conflict of interest There is no conflict of interest.

Ethical approval All procedures performed in studies involving human participants were under the ethical standards of the institutional and/or national research committee and with the 1964 Helsinki declaration and its later amendments or comparable ethical standards.

Informed consent It was obtained from all individual participants included in the study.

References

1. Jemal A, Bray F, Center MM, Ferlay J, Ward E, Forman D. Global cancer statistics. CA Cancer J Clin. 2011;61:69–90.
2. Delaney G, Jacob S, Featherstone C, Barton M. The role of radiotherapy in cancer treatment: estimating optimal utilization from a review of evidence based clinical guidelines. Cancer. 2005;104:1129–37.
3. Early Breast Cancer Trialists' Collaborative Group. Effect of radiotherapy after breast-conserving surgery on 10-year recurrence and 15-year breast cancer death: meta-analysis of individual patient data for 801 women in 17 randomized trials. Lancet. 2011;378:1707–16.
4. Rattay T, Talbot C. Finding the genetic determinants of adverse reactions to radiotherapy. Clin Oncol (R Coll Radiol). 2014;26:301–8.
5. West CM, Barnett GC. Genetics and genomics of radiotherapy toxicity: towards prediction. Genome Med. 2011;3:52.
6. Kuo SH, Huang CS. Association between radiosensitivity and molecular subtypes in patients with early-stage breast cancer and lymph node-negative status. Trans Cancer Res. 2017;1(6):9.
7. Meattini I, Francolini G, Livi L. Radiosensitivity in the breast cancer management scenario: another step forward? J Thorac Dis. 2016;8(10):E1361.
8. De Ruyck K, de Gelder V, Van Eijkeren M, Boterberg T, De Neve W, Vral A, et al. Chromosomal radiosensitivity in head and neck cancer patients: evidence for genetic predisposition? Br J Cancer. 2008;98:1723–38.
9. Scott D, Barber JBP, Spreadborough AR, Burril W, Roberts SA. Increased chromosomal radiosensitivity in breast cancer patients: a comparison of the two assays. Int J Radiat Biol. 1999;75:1–10.
10. Baeyens A, Thierens H, Claes K, Poppe B, Messiaen L, De Ridder L, Vral A. Chromosomal radiosensitivity in breast cancer patients with a known or putative genetic predisposition. Br J Cancer. 2002;87:1379–85.
11. Terzoudi GI, Hatzi VI, Barszczewska K, Manola KN, Stavropoulou C, Angelakis P, et al. G2-checkpoint abrogation in irradiated lymphocytes: A new cytogenetic approach to assess individual radiosensitivity and predisposition to cancer. Int J Oncol. 2009;35:1223–30.
12. Parshad R, Sanford KK, Jones GM. Chromatid damage after G2 phase x-irradiation of cells from cancer-prone individuals implicates deficiency in DNA repair. Proc Natl Acad Sci U S A. 1983;80:5612–26.
13. Mozdarani H, Bryant PE. Kinetics of chromatid aberrations in G2 ataxia- telangiectasia cells exposed to X-rays and ara A. Int J Radiat Biol. 1989;55:71–84.

14. Mahmoodi M, Abolhassani H, Mozdarani H, Rezaei N, Azizi G, et al. *In vitro* chromosomal radiosensitivity in patients with common variable immunodeficiency. Cent Eur J Immunol. 2018;43:155–61.
15. Mozdarani H, Kiaee F, Fekrvand S, Azizi G, Yazdani R, et al. G2-lymphocyte chromosomal radiosensitivity in patients with LPS responsive beige-like anchor protein (LRBA) deficiency. Int J Radiat Biol. 2019;95:680–90.
16. Amirifar P, Mozdarani H, Yazdani R, Kiaei F, Moeini Shad T, et al. Effect of class switch recombination defect on the phenotype of ataxia-telangiectasia patients. Immunol Invest. 2020;50:1–15.
17. Scott D. Chromosomal radiosensitivity, cancer predisposition and response to radiotherapy. Strahlenther Onkol. 2000;176:229–34.
18. Mozdarani H, Ziaee Mashhadi AH, Alimohammadi Z. G2 chromosomal radio sensitivity and background frequency of sister chromatid exchanges of peripheral blood lymphocytes of breast cancer patients. Int J Radiat Res. 2011;9:167–74.
19. Mozdarani H, Salimi M, Bakhtari N. Inherent radiosensitivity and its impact on breast cancer chemo-radiotherapy. Int J Radiat Res. 2017;15(4):325–41.
20. Vignard J, Mirey G, Salles B. Ionizing-radiation induced DNA double-strand breaks: a direct and indirect lighting up. Radiother Oncol. 2013;108:362–9.
21. Löbrich M, Jeggo P. A process of resection-dependent nonhomologous end joining involving the goddess artemis. Trends Biochem Sci. 2017;42:690–701.
22. Bryant PE. Mechanisms of radiation-induced chromatid breaks. Mutat Res. 1998;404:107–11.
23. Bryant PE, Mozdarani H. Mechanisms underlying the conversion of DNA double-strand breaks into chromatid breaks. Mutat Res. 2010;701:23–6.
24. Liu X, Li F, Huang Q, Zhang Z, Zhou L, et al. Self-inflicted DNA double-strand breaks sustain tumorigenicity and stemness of cancer cells. Cell Res. 2017;27:764–83.
25. Jackson SP, Bartek J. The DNA-damage response in human biology and disease. Nature. 2009;461:1071–8.
26. Lin J, Cai D, Li W, Yu T, Mao H, Jiang S, Xiao B. Plasma circular RNA panel acts as a novel diagnostic biomarker for colorectal cancer. Clin Biochem. 2019;74:60–8.
27. Zheng Q, Bao C, Guo W, Li S, Chen J, Chen B, Luo Y, Lyu D, Li Y, Shi G, Liang L. Circular RNA profiling reveals an abundant circHIPK3 that regulates cell growth by sponging multiple miRNAs. Nat Commun. 2016;7:1–3.
28. Fan X, Yang Y, Chen C, Wang Z. Pervasive translation of circular RNAs driven by short IRES-like elements. Nat Commun. 2022;13:1–5.
29. Kristensen LS, Jakobsen T, Hager H, Kjems J. The emerging roles of circRNAs in cancer and oncology. Nat Rev Clin Oncol. 2022;19:188–206.
30. Liu B, Dong X, Cheng H, Zheng C, Chen Z, Rodríguez TC, et al. A split prime editor with untethered reverse transcriptase and circular RNA template. Nat Biotechnol. 2022;4:1–6.
31. Attwaters M. *In vivo* RNA base editing with circular RNAs. Nat Rev Genet. 2022;23:196–7.
32. He J, Xie Q, Xu H, Li J, Li Y. Circular RNAs and cancer. Cancer Lett. 2017;396:138–44.
33. Nielsen AF, Bindereif A, Bozzoni I, Hanan M, Hansen TB, Irimia M, et al. Best practice standards for circular RNA research. Nat Methods. 2022;26:1–3.
34. Yang Z, Huang C, Wen X, Liu W, Huang X, Li Y, Zang J, et al. Circular RNA circ-FoxO3 attenuates blood-brain barrier damage by inducing autophagy during ischemia/reperfusion. Mol Ther. 2022;30:1275–87.
35. Zhou J, Zhou LY, Tang X, Zhang J, Zhai LL, Yi YY, et al. Circ-Foxo3 is positively associated with the Foxo3 gene and leads to better prognosis of acute myeloid leukemia patients. BMC Cancer. 2019;19:1–1.
36. Kong Z, Wan X, Lu Y, Zhang Y, Huang Y, Xu Y, et al. Circular RNA circFOXO3 promotes prostate cancer progression through sponging miR-29a-3p. J Cell Mol Med. 2020;24:799–813.
37. Zhang Y, Ge P, Zhou D, Xing R, Bai L. Circular RNA FOXO3 accelerates glycolysis and improves cisplatin sensitivity in lung cancer cells via the miR-543/Foxo3 axis. Oncol Lett. 2021;22:1.
38. Nair AA, Niu N, Tang X, Thompson KJ, Wang L, Kocher JP, et al. Circular RNAs and their associations with breast cancer subtypes. Oncotarget. 2016;7:80967.
39. Smit L, Berns K, Spence K, Ryder WD, Zeps N, Madiredjo M, et al. An integrated genomic approach identifies that the PI3K/AKT/FOXO pathway is involved in breast cancer tumor initiation. Oncotarget. 2016;7:2596.
40. Du WW, Fang L, Yang W, Wu N, Awan FM, Yang Z, et al. Induction of tumor apoptosis through a circular RNA enhancing Foxo3 activity. Cell Death Differ. 2017;24:357–70.
41. Wang C, Tao W, Ni S, Chen Q. Circular RNA circ-Foxo3 induced cell apoptosis in urothelial carcinoma via interaction with miR-191-5p. Onco Targets Ther. 2019;12:8085.
42. Kong Z, Wan X, Lu Y, Zhang Y, Huang Y, Xu Y, Liu Y, et al. Circular RNA circFOXO3 promotes prostate cancer progression through sponging miR-29a-3p. J Cell Mol Med. 2020;24:799–813.
43. Qiu Y, Xie X, Lin L. circFOXO3 protects cardiomyocytes against radiation-induced cardiotoxicity. Mol Med Rep. 2021;23:177.
44. Xing Y, Zha WJ, Li XM, Li H, Gao F, Ye T, et al. Circular RNA circ-Foxo3 inhibits esophageal squamous cell cancer progression via the miR-23a/PTEN axis. J Cell Biochem. 2020;121:2595–605.
45. Wang N, Tan HY, Feng YG, Zhang C, Chen F, Feng Y. microRNA-23a in human cancer: its roles, mechanisms and therapeutic relevance. Cancers (Basel). 2018;11:7.
46. Wang N, Zhu M, Tsao SW, Man K, Zhang Z, Feng Y. MiR-23a-mediated inhibition of topoisomerase 1 expression potentiates cell response to etoposide in human hepatocellular carcinoma. Mol Cancer. 2013;12:1. https://doi.org/10.1186/1476-4598-12-119.
47. Li J, Aung LH, Long B, Qin D, An S, Li P. miR-23a binds to p53 and enhances its association with miR-128 promoter. Sci Rep. 2015;5:1–3. https://doi.org/10.1038/srep16422.
48. Chen G, Li Y, He YI, Zeng B, Yi C, Wang C, et al. Upregulation of circular RNA circATRNL1 to sensitize oral squamous cell carcinoma to irradiation. Mol Ther Nucleic Acids. 2020;19:961–73.
49. Jia-Quan Q, Hong-Mei Y, Xu Y, Li-Na L, Jin-Feng Z, Ta X, et al. MiR-23a sensitizes nasopharyngeal carcinoma to irradiation by targeting IL-8/Stat3 pathway. Oncotarget. 2015;6:28341.
50. Zheng Y, Liu L, Chen C, Ming P, Huang Q, Li C, et al. The extracellular vesicles secreted by lung cancer cells in radiation therapy promote endothelial cell angiogenesis by transferring miR-23a. PeerJ. 2017;5: e3627.
51. Barnett G, Wilkinson J, Moody A, Wilson C, Twyman N, et al. The Cambridge breast intensity-modulated radiotherapy trial: patient-and treatment-related factors that influence late toxicity. Clin Oncol (R Coll Radiol). 2011;23:662–73.
52. Ernestos B, Nikolaos P, Koulis G, Eleni R, Konstantinos B, et al. Increased chromosomal radiosensitivity in women carrying BRCA1/BRCA2 mutations assessed with the G2 assay. Int J Radiat Oncol Biol Phys. 2010;76:1199–205.
53. Terzoudi ITJ, Hain J, Vrouvas J, Margaritis K, Donta-Bakoyianni C, et al. Increased G2 chromosomal radiosensitivity in cancer patients: the role of cdk1/cyclin-B activity level in the mechanisms involved. Int J Radiat Biol. 2000;76:607–15.
54. Riches A, Bryant P, Steel C, Gleig A, Robertson A, et al. Chromosomal radiosensitivity in G 2-phase lymphocytes identifies

breast cancer patients with distinctive tumour characteristics. Br J Cancer. 2001;85:1157–61.
55. Scott D, Spreadborough A, Levine E, Roberts SA. Genetic predisposition in breast cancer. Lancet. 1994;344:1444.
56. Wang W, Luo YP. MicroRNAs in breast cancer: oncogene and tumor suppressors with clinical potential. J Zhejiang Univ Sci B. 2015;16:18–31.
57. Zhang Y, Zhao H, Zhang L. Identification of the tumor-suppressive function of circular RNA FOXO3 in non-small cell lung cancer through sponging miR-155. Mol Med Rep. 2018;17:7692–700.
58. Lu M, Zhao Y, Xu F, Wang Y, Xiang J, Chen D. The expression and prognosis of FOXO3a and Skp2 in human ovarian cancer. Med Oncol. 2012;29:3409–15.
59. Zhou J, Zhou LY, Tang X, Zhang J, Zhai LL, Yi YY, et al. Circ-Foxo3 is positively associated with the Foxo3 gene and leads to better prognosis of acute myeloid leukemia patients. BMC Cancer. 2019;19:930.
60. Shen Z, Zhou L, Zhang C, Xu J. Reduction of circular RNA Foxo3 promotes prostate cancer progression and chemoresistance to docetaxel. Cancer Lett. 2020;468:88–101.
61. Chen P, He YH, Huang X, Tao SQ, Wang XN, Yan H, et al. MiR-23a modulates X-linked inhibitor of apoptosis-mediated autophagy in human luminal breast cancer cell lines. Oncotarget. 2017;8:80709.
62. Ma F, Li W, Liu C, Li W, Yu H, Lei B, et al. MiR-23a promotes TGF-β1-induced EMT and tumor metastasis in breast cancer cells by directly targeting CDH1 and activating Wnt/β-catenin signaling. Oncotarget. 2017;8:69538.
63. Chen G, Li Y, He YI, Zeng B, Yi C, Wang C, et al. Upregulation of circular RNA circATRNL1 to sensitize oral squamous cell carcinoma to irradiation. Mol Ther Nucleic Acids. 2010;19:961–73.
64. Tsai YS, Lin CS, Chiang SL, Lee CH, Lee KW, Ko YC. Areca nut induces miR-23a and inhibits repair of DNA double-strand breaks by targeting FANCG. Toxicol Sci. 2011;123:480–90.
65. Borgmann K, Röper B, Abd El-Awady R, Brackrock S, Bigalke M, Dörk T, et al. Indicators of late normal tissue response after radiotherapy for head and neck cancer: fibroblasts, lymphocytes, genetics, DNA repair, and chromosome aberrations. Radiother Oncol. 2002;64:141–52.
66. Li Y, Ma L. Efficacy of chemotherapy for lymph node-positive luminal A subtype breast cancer patients: an updated meta-analysis. World J Surg Oncol. 2020;18:1–1.
67. Negi P, Kingsley PA, Jain K, Sachdeva J, Srivastava H, Marcus S, et al. Survival of triple negative versus triple positive breast cancers comparison and contrast. Asian Pac J Cancer Prev. 2016;17:3911–6.
68. Jang Y, Jung H, Kim HN, Seo Y, Alsharif E, Nam SJ, et al. Clinicopathologic characteristics of HER2-positive pure mucinous carcinoma of the breast. J Pathol Transl Med. 2020;54:95–102.
69. Rao D, Yu C, Sheng J, Lv E, Huang W. The Emerging Roles of circFOXO3 in Cancer. Front Cell Dev Biol. 2021;9:659417.
70. Yang W, Du WW, Li X, Yee AJ, Yang BB. Foxo3 activity promoted by non-coding effects of circular RNA and Foxo3 pseudogene in the inhibition of tumor growth and angiogenesis. Oncogene. 2016;35:3919–31.
71. Oikawa S, Wada S, Lee M, Maeda S, Akimoto T. Role of endothelial microRNA-23 clusters in angiogenesis *in vivo*. Am J Physiol Heart Circ Physiol. 2018;315:H838–46.